



Citation for published version:

Hari, M, Wang, K, Bending, SJ, Arac, E, Atkinson, D, Lepadatu, S, Claydon, JS & Marrows, CH 2013, 'Current-driven domain wall motion in artificial magnetic domain structures', *Journal of the Korean Physical Society*, vol. 62, no. 10, pp. 1534-1538. <https://doi.org/10.3938/jkps.62.1534>

DOI:

[10.3938/jkps.62.1534](https://doi.org/10.3938/jkps.62.1534)

Publication date:

2013

Document Version

Peer reviewed version

[Link to publication](#)

University of Bath

Alternative formats

If you require this document in an alternative format, please contact:
openaccess@bath.ac.uk

General rights

Copyright and moral rights for the publications made accessible in the public portal are retained by the authors and/or other copyright owners and it is a condition of accessing publications that users recognise and abide by the legal requirements associated with these rights.

Take down policy

If you believe that this document breaches copyright please contact us providing details, and we will remove access to the work immediately and investigate your claim.

Current-driven domain wall motion in artificial magnetic domain structures

M. Hari, K. Wang, S.J. Bending

Department of Physics, University of Bath, Claverton Down, Bath BA2 7AY, UK

E. Arac, D. Atkinson

Department of Physics, Durham University, Durham DH1 3LE, UK

S. Lepadatu, J.S. Claydon, C.H. Marrows

School of Physics and Astronomy, University of Leeds, Leeds LS2 9JT, UK

We report progress towards optimisation of artificial magnetic domain structures for efficient spin transfer torque domain wall (DW) motion. Co/Pt multilayer samples have been sputtered on (100) Si/SiO₂ substrates and perpendicular magnetic anisotropy confirmed using polar magneto-optical Kerr effect (MOKE) measurements. The influence of the thickness of Co and Pt layers on the coercivity and switching behaviour was systematically investigated and the conditions established for realising well-suited structures with medium coercivity (~100 Oe) and sharp switching fields. Optimised Co/Pt multilayer films have been lithographically patterned into nanowire devices for time-resolved extraordinary Hall effect (EHE) measurements. Our devices are based on 50 Ω coplanar waveguides incorporating single and double Hall cross structures. The coercivity of the region surrounding the Co/Pt Hall crosses was reduced by local focussed ion beam (FIB) irradiation allowing the controlled nucleation of domain walls at the edges of these regions by application of an appropriate field sequence. We describe polar MOKE experiments that show how DC currents lead to asymmetric switching of these artificial domains due to current-assisted DW motion across them.

PACS number: 75.76.+j, 75.47.-m, 75.30.Gw

Keywords: Domain wall motion, Coercivity

Email: M.Hari@bath.ac.uk

Control, Extraordinary Hall Effect

Fax: +44-1225 386110

I. INTRODUCTION

Continued rapid advances in information technology are driving an increasing need to develop new forms of non-volatile magnetic memory devices. Spintronics is an emerging technology that exploits both the charge and the spin magnetic moment of electrons. Recent efforts to generate and utilize spin polarised currents to control domain wall dynamics in ferromagnetic structures have led to several breakthroughs [1]. However, the current densities required to achieve spin transfer torque (STT) wall motion [2-6] are currently still too high ($1\text{-}5 \times 10^8 \text{A/cm}^2$) for practical applications. We have recently developed and investigated “artificial domain structures” based on the local focused ion beam (FIB) irradiation of magnetic multilayer structures with perpendicular magnetic anisotropy [7-9]. This approach allows us to define nanoscale ferromagnetic domains of arbitrary shape with controllable anisotropy and coercive fields. We are now exploring implementation of artificial magnetic domains to optimise structures for STT domain wall motion. Not only do these eliminate the need for an additional field pulse to nucleate a domain wall, but the ability to tune the local magnetic anisotropy represents an additional control parameter that can be used to reduce critical current densities.

The use of FIB irradiation is a well established technique (10) for controlling the magnetic properties of systems with perpendicular magnetic anisotropy (PMA). In earlier work we have studied PMA in Pt/Co/Pt trilayers, with Co thickness less than 1nm [8]. The strength of PMA in these structures is influenced by the interface roughness, strain and the intermixing at the Co-Pt interfaces [11-13]. Ga^+ FIB irradiation tends to relax the strain at interfaces, resulting in a reduction of the film coercivity [14]. In this way artificial domains can be realised formed from adjacent regions with very similar magnetisation but different coercive fields, presenting a novel opportunity to reduce the current density for STT DW motion.

II. EXPERIMENTAL METHOD

Pt(1.8nm)/Co(0.45nm)/Pt(3nm) thin films were grown using magnetron sputtering onto Si/SiO₂(90nm) substrates (Fig 1). The base pressure of the sputtering system was 1.4×10^{-7} mTorr and the Ar pressure during sputtering was 2.5 mTorr. Good PMA was realised in Pt/Co/Pt multilayer stacks with Co thicknesses ranging from 0.3 – 0.7 nm (Fig 2). Upon increasing the Co thickness further the magnetization reverts to the in-plane direction. 5mm×5mm chips were diced from larger pieces of wafer and patterned into 2µm wide Hall cross structures using optical lithography and Ar-ion milling. Cr/Au contacts, designed to form a 50Ω coplanar waveguide structure, were defined by evaporation and lift-off (Fig 3). The top Pt layer is very thin making the structure extremely sensitive to irradiation and a 4nm of Si film was deposited on the top of the Hall Cross and oxidised in air to act as a suppression layer reducing the energy and dose levels of the FIB Ga⁺ ions when they reach the Co/Pt interfaces.

A low frequency EHE setup, with current and voltage leads connected to a single Hall cross, was constructed to characterise the magnetotransport properties of completed structures. The device is placed inside a cylindrical coil connected to a regulated bipolar power supply to generate controlled magnetic field cycles with the field normal to the plane of the sample. The Hall cross is driven with a constant (32Hz) ac current in the range 1-7µA from a function generator and the Hall voltage signal obtained is detected using a lock-in amplifier. The entire experiment is controlled with LabView allowing arbitrarily complex field histories to be explored. The measured magnetotransport data have been compared with independent high sensitivity polar MOKE measurements with a laser beam diameter of approximately 5µm and a 27Hz oscillating magnetic field. Polar MOKE measurements also allow the ready application of dc and pulsed transport currents to study the influence of an additional STT.

True time-of-flight EHE measurements are possible by modifying our low frequency magnetotransport apparatus as shown in Figure 4. A fast pulse generator is used to drive current through the sample and the Hall voltage pulse detected using a differential probe into a 6GHz digital signal analyser. A quasi-static magnetic field is used to nucleate DWs prior to the application of the current pulse, elegantly separating the generation and motion of DWs.

III. RESULTS & DISCUSSION

Following the experimental method described above we have fabricated linear arrays of five $2\mu\text{m}\times 2\mu\text{m}$ Hall crosses on a $3.75\times 3.75\text{mm}$ chip, for calibrating the Ga^+ dose-dependence of the magnetic properties of our multilayers. Figure 5 shows a set of EHE hysteresis loops as a function of irradiation dose measured at 300 K on the Hall array sample. In all cases an area of about $20\mu\text{m}\times 10\mu\text{m}$ was irradiated around the active cross structures. The EHE measurements yield information about the coercivity and perpendicular magnetic anisotropy of the Pt/Co/Pt sandwich structures and allow a comparison of the dosed and undosed elements in order to select optimum irradiation doses for experiments. The undosed Hall cross has an almost square hysteresis loop compared to the irradiated ones which become increasingly more rounded with dose. It is evident from Fig. 5 that the samples tend to lose PMA as the Ga^+ dose is increased, and the magnetisation in the samples with $0.011\text{ pC}/\mu\text{m}^2$ and $0.014\text{ pC}/\mu\text{m}^2$ appears to have reverted to the in-plane direction. This is due to the fact that, as the FIB dose increases, the PMA due to interface anisotropy becomes suppressed and bulk in-plane anisotropy starts to dominate. Calibration measurements of this type yield the precise dose level of the FIB Ga^+ ions needed to optimise samples for t-resolved EHE measurements.

Figure 6 shows low frequency EHE data from a single $2\mu\text{m}$ wirewidth Hall cross connected via a 50Ω Cr/Au co-planar waveguide structure. A $20\mu\text{m}\times 10\mu\text{m}$ region

asymmetrically positioned (extending $5\mu\text{m}$ from the centre in one direction and $15\mu\text{m}$ in the other) along the current lead direction was irradiated with a dose level of $0.004\text{ pC}/\mu\text{m}^2\text{ Ga}^+$ ions. The two EHE plots before and after irradiation confirm [15-16] that an artificial domain can be created around the Hall cross due to the reduced coercivity of this region. To corroborate these results and make preliminary studies with applied dc currents, we have investigated the same sample using a polar MOKE set-up. The $5\mu\text{m}$ laser spot size allowed us to probe magnetisation reversal in several different locations on the sample, both irradiated and unirradiated regions, with and without a bias current. Figures 7a, b without a dc bias current, reveal that the MOKE magnetisation loops are both symmetric with a much larger coercive field in unirradiated regions (7a) than in irradiated regions (7b).- Figures 8 a, b illustrate the influence of the application of $+50\text{ }\mu\text{A}$ (8a) or $-50\text{ }\mu\text{A}$ (8b) dc currents.- A small field-dependent offset of the coercive fields arises with an applied dc current that depends on the direction of electron flow. Assuming that the measured coercive field is dominated by the closest artificial DW to the Hall cross, we presume that this reflects a STT that accelerates DW motion and reversal for one current direction and suppresses it for the other.

IV. CONCLUSION

Co/Pt multilayer films have been grown using magnetron sputtering and strong PMA achieved for small Co thicknesses. Optimised Hall effect structures comprising Pt/Co/Pt trilayers were micropatterned on 5mm and 3.75mm chips using optical lithographic techniques and artificial magnetic domains realised using Ga^+ FIB irradiation. The use of FIB irradiation allows us to precisely control the local coercivity and anisotropy of the domains. Low frequency EHE measurements were used to characterise the magnetic properties of unirradiated and irradiated samples, allowing us to calibrate the FIB irradiation dose required

to realise optimised structures for STT experiments. The same structures were also investigated with polar MOKE, allowing the influence of additional dc currents to be studied. These preliminary MOKE results suggest the existence of a current-driven STT that breaks the symmetry of the magnetic hysteresis curves. A time-resolved EHE measurement setup has also been designed and built to measure the transient Hall voltage due to the application of current pulses in static magnetic fields. This will be used in the near future to investigate the real-time motion of DWs in our structures.

REFERANCES

- [1] S.S.P. Parkin, US Patents Nos. 6.834.005, 6.898.132, 6.920.062, 7.031.178 & 7.236.386 (2004-2007).
- [2] Hayashi *et al.*, PRL **96**, 197207 (2006).
- [3] Hayashi *et al.*, PRL **97**, 207205 (2006).
- [4] Thomas *et al.*, Nature **443**, 197 (2006).
- [5] Hayashi *et al.*, Nature Physics **3**, 21 (2007).
- [6] Hayashi *et al.*, PRL **98**, 037204 (2007).
- [7] S.Hashimoto *et al.*, J. Appl. Phys. **67**, 4429 (1990)
- [8] C.Chappert *et al.*, Science **280**, 1919 (1998) ;
- [9] T.Devolder *et al.*, Appl. Phys. Lett. **74**, 3383 (1999).
- [10] J.Fassbender *et al.*, J. Phys D: Appl. Phys. **37**, R179 (2004).
- [11] S.Hashimoto *et al.*, J. Appl. Phys. **67**, 4429 (1990).
- [12] C.Chappert *et al.*, Science **280**, 1919 (1998);
- [13] T.Devolder *et al.*, Appl. Phys. Lett. **74**,3383 (1999).
- [14] C. Vieu, J. Gierak, H. Launois, T. Aign, P. Meyer, J. P. Jamet, J. Ferre, C. Chappert, T. Devolder, V. Mathet, and H. Bernas, J. Appl. Phys. **91**, 3103 (2002).
- [15] K. Wang, M-C. Wu, S. Lepadatu, J. S. Claydon, C.H. Marrows, and S. J. Bending, J.

Appl. Phys. **110**, 083913 (2011).

[16] A. Aziz, S. J. Bending, H. Roberts, S. Crampin, P. J. Heard, and C. H. Marrows, J. Appl. Phys. **98**, 124102 (2005).

ACKNOWLEDGEMENTS

This work was supported in the UK by EPSRC under grant No. EP/G010897/1.

Figure Captions

Figure 1: Ultra-thin 0.45nm Co layer in sputtered Pt/Co/Pt sandwich structures

Figure 2: MOKE data before device processing for Pt(3.0)/Co(0.45)/Pt(1.8) nm films.

Figure 3: Optical lithography and FIB irradiation processes.

Figure 4: Schematic diagram of setup for time-resolved EHE measurement

Figure 5: FIB dose calibration of Hall array. H_{c0} is the coercive field of the unirradiated reference sample.

Figure 6: low frequency EHE measurement of a $2\mu\text{m}$ Hall cross FIB irradiated at a dose of $0.004\text{ pC}/\mu\text{m}^2$ $-\text{Ga}^+$ ions. H_{c0} is the coercive field of the unirradiated reference sample.

Figure 7a & 7b: Preliminary MOKE results without a dc bias current, where magnetisation loops are both symmetric with a much larger coercive field in unirradiated regions (7a) than in irradiated regions (7b). H_{c0} is the coercive field of the unirradiated reference sample.

Figure 8a & 8b: MOKE data with a $\pm 50\text{ }\mu\text{A}$ dc current applied when the loop becomes systematically offset

- with offset direction dependent on the direction of electron flow. H_{c0} is the coercive field of the unirradiated reference sample.

Fig. 1

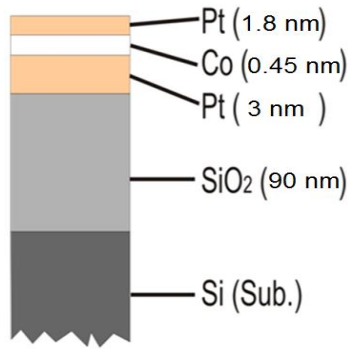


Fig. 2

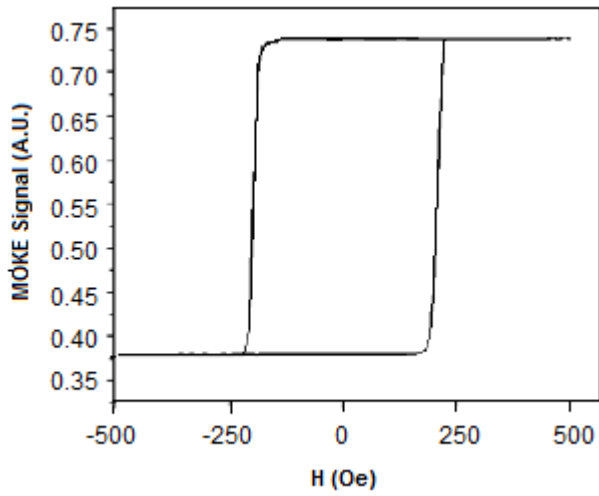


Fig. 3

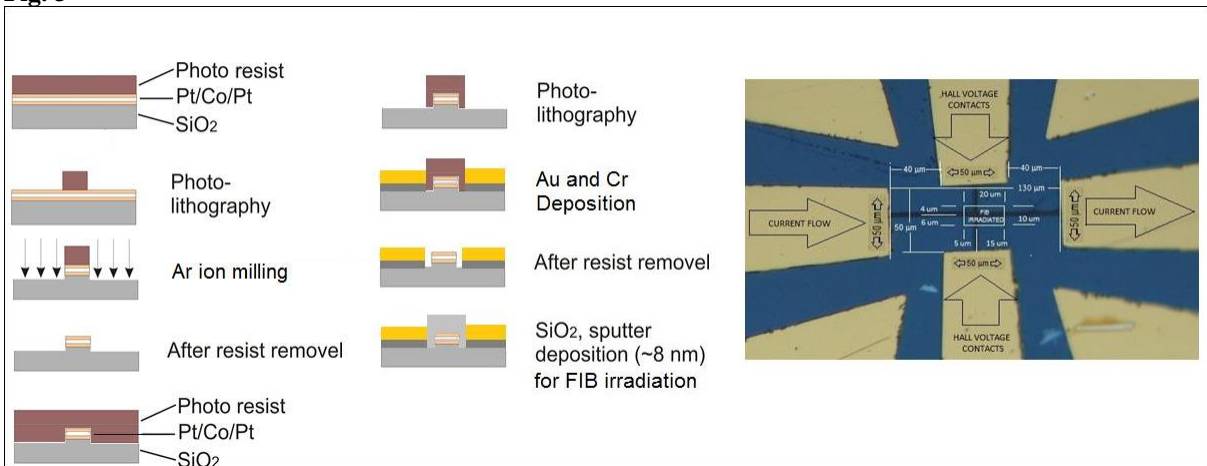


Fig. 4

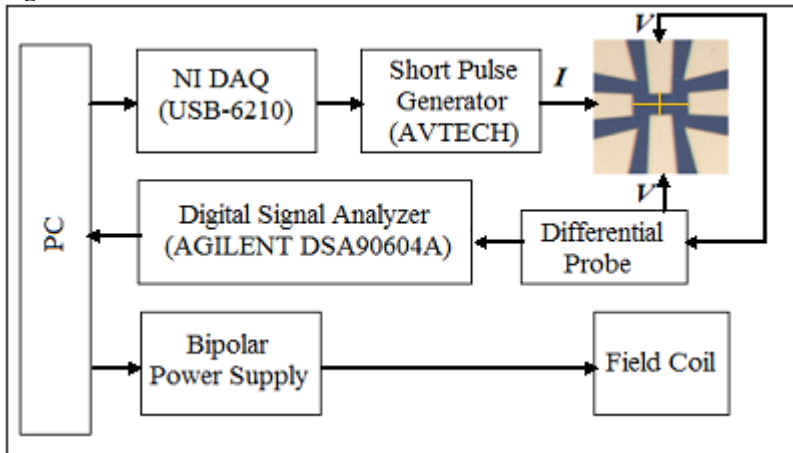


Fig. 5

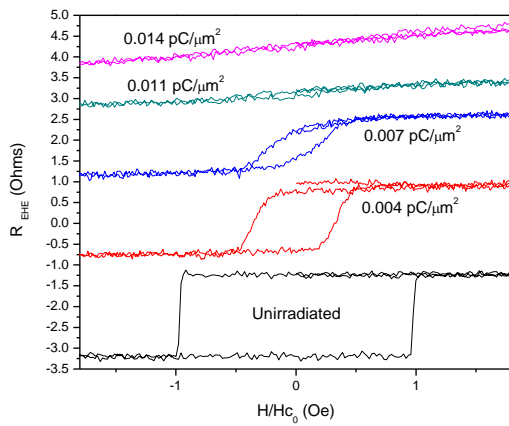


Fig. 6

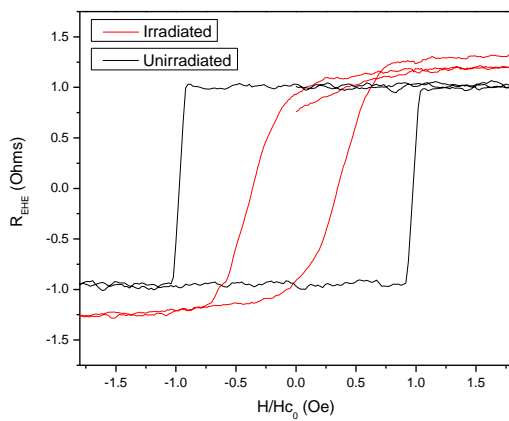


Fig. 7a

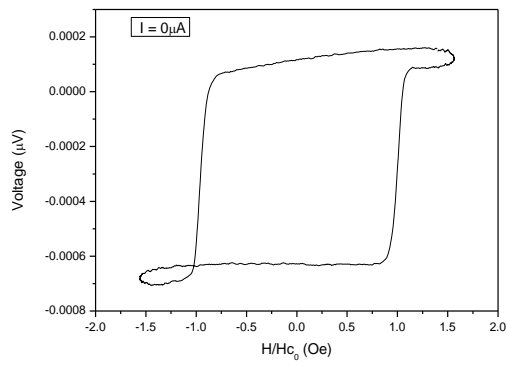


Fig. 7b

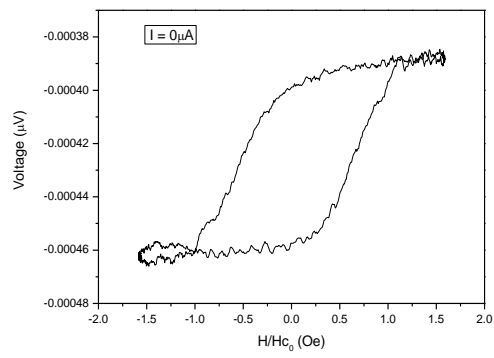


Fig. 8a

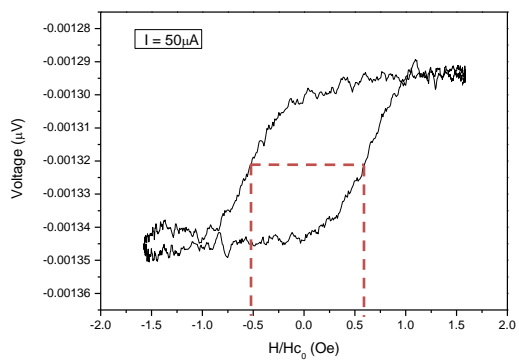


Fig. 8b

